ISSN 1069-3513, Izvestiya, Physics of the Solid Earth, 2011, Vol. 47, No. 1, pp. 59–71. © Pleiades Publishing, Ltd., 2011.
Original Russian Text © N.N. Nevedrova, E.V. Pospeeva, A.M. Sanchaa, 2011, published in Fizika Zemli, 2011, No. 1, pp. 63–75.

Interpretation of Complex Electromagnetic Data in Seismically Active Regions: Case Study of the Chuya Depression, Mountain Altai

N. N. Nevedrova, E. V. Pospeeva, and A. M. Sanchaa

Trofimuk Institute of Petroleum Geology and Geophysics, Siberian Branch, Russian Academy of Sciences, pr. Akad. Koptyuga 3, Novosibirsk, 630090 Russia

Received January 12, 2010

Abstract—A procedure for the simultaneous interpretation of magnetotelluric and near-field transient electromagnetic sounding (MTS and NF TEMS, respectively) data is proposed. The advantages of the complex interpretation are demonstrated by specific examples. In accordance with the interpretation of the field data, geoelectrical sections of the lithosphere in the western part of the Chuya Depression are constructed. A reduction in the depth to the conductive crustal layer in the epicentral zone is found, and the geoelectrical boundary in the upper part of the paleozoic basement is revealed.

DOI: 10.1134/S1069351311010083

INTRODUCTION

The Institute of Petroleum Geology and Geophysics, Siberian Branch, Russian Academy of Sciences, is carrying out complex geological and geophysical surveys in the Mountain Altai. These studies were considerably expanded after the destructive Chuya earthquake with a magnitude of 7.5 on the Richter scale that occurred on September 27, 2003. This was the strongest event over the instrumental period of seismological observations. The focal zone of the earthquake overlaps the territory of the Chuya and Kurai Depressions, and the North Chuya Range. The main earthquake rupture is well observed in the western part of the Chuya Depression as a discontinuous belt of local fractures, landslides, and ground displacements. It was decided to carry out a complex electromagnetic survey over a test area in the western closure of the Chuya Depression, where the array electromagnetic measurements with controlled and natural sources were deployed (Fig. 1).

Since no magnetotelluric sounding (MTS) had been carried out in the Mountain Altai until recently, the main goal of our study was to reconstruct the deep geoelectric cross section of the lithosphere according to the MTS data, and to refine the structure of the sedimentary cover and the upper portion of the paleozoic basement using a complex of MTS and near-field transient electromagnetic sounding (NF TEMS) methods.

The present work also addresses another challenging issue, which is urgent for all seismically active regions including the Mountain Altai. It is studying the time dynamics of the geoelectrical parameters of a rock massif that underwent strong seismic impact [Nevedrova, 2007]. There is a considerable amount of archival electric data to support modern studies. These data include vertical electric sounding (VES) and NF TEMS results obtained for the Altai depressions in the latter half of the 20th century. These data were used to determine the geoelectrical parameters of the environment before the destructive earthquake of 2003.

The efficiency of the electromagnetic monitoring of geodynamical processes undoubtedly depends on the detailed studies of the geoelectric structure to which the present paper is primarily devoted.

FIELD TECHNIQUE

The controlled-source electromagnetic sounding (NF TEMS and VES) were carried out in the western part of the Chuya Depression in a set of profiles (Fig. 1). Figure 1 depicts the profiles and observation sites of all electromagnetic measurements. NF TEMS measurements were implemented as the sounding with induction excitation of the field and recording the time derivative of the vertical component of the magnetic field ($\partial Hz/\partial t$) in the coaxial loop configuration. We note that in case of induction excitation and recording, the high-resistivity screens have no effect, and the influence of local near-surface heterogeneities is weak. These factors are also important in the field measurements on the territory of intermontane tectonic troughs, where the upper part of the cross section contains insular permafrost and lenses of coarse-grained deposits. The side length of the transmitter loop was 400 m, and the same was the spacing of measurement sites. The average distance between NF TEMS profiles was 2–4 km.

Based on the geophysical interpretation, it has been established earlier that the controlled-source electromagnetic methods in the geological conditions of the Mountain Altai provide an exploration depth of

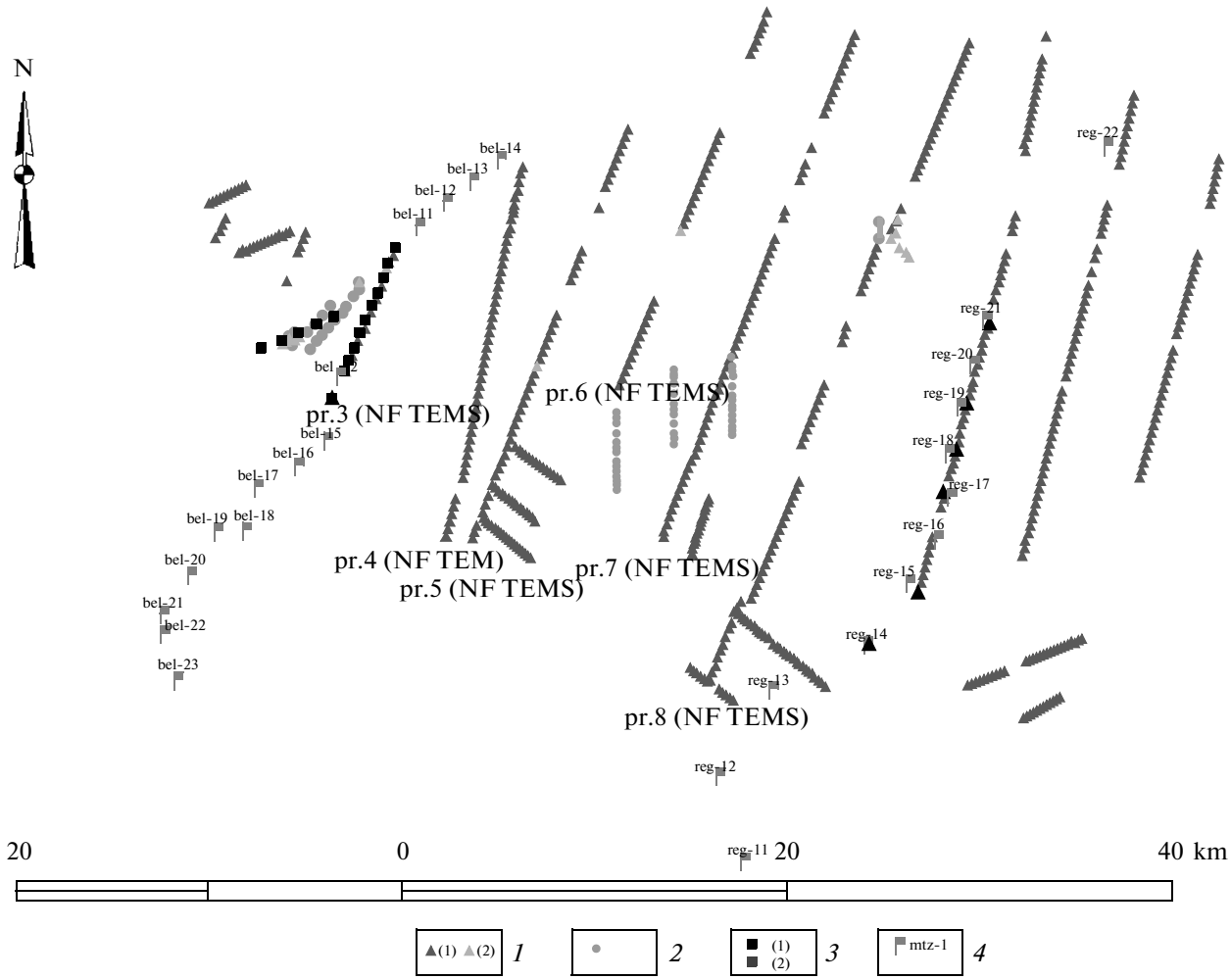

Fig. 1. The map of the actual surveys. Profiles and sites of electomagnetic observations in the western part of the Chuya Depression: *1* NF TEMS sites, archival and present-day; *2* VES sites; *3* MTS 2007–2008 sites, present-day and acquired by the Krasnoyarsk Research Institute of Geology and Mineral Resources; *4* MTS sites, 2009.

up to 1–2 km. In order to increase the depth of investigation and the informativeness of the geoelectrical studies in the epicentral zone of a large earthquake, an average-scale MTS survey was carried out over the range of periods from 0.003 to 6000 s. These MTS measurements were conducted using the new-generation MTU–System–2000 (Phoenix Geophysics, Canada) equipment provided with the software for raw data processing (Satellite Synchronized MT, the SSMT).

An extended MTS profile was acquired in the western part of the Chuya Depression. The profile starts in the southwest mountain framing of the depression, the South Chuya Range, and ends in its northern part, in the region of the Chagan–Uzun massif. The measurements were carried out at 23 stations with an average spacing of 2 km. In the zone of tectonic deformations of the earthquake the distance between the MT sites was reduced to 1 km; the MTS stations in this region were coincident with the NF TEMS sites.

Rectangular receiving setups consisting of grounded receiving lines E_x, E_y, and three magnetic sensors H_x, H_y, and H_z were used for registration of magnetotelluric variations. The length of the receiving electric lines was 100 m. This is the most suitable length providing optimal signal-to-noise ratio in the survey region. The time of recording was 19–22 h.

PROCESSING AND INTERPRETATION OF THE COMPLEX EM DATA

Near-Field TEM Data

At the first stage of processing, the field NF TEM data acquired in the observation profiles was considered. The entire volume of measurements was analyzed; each apparent resistivity curve was analyzed individually. The quality of measurements and possible data corruption were assessed; the character of the changes in the resistivity curves along the profile and their correlation with each other were analyzed; and

the main regularities in the transient process at different segments of the profile were revealed. Then, the entire volume of the NF TEM field data was processed using the interactive computer systems for interpretation and computer modeling of nonstationary electromagnetic fields. Two automated systems—ERA and EMS program complexes, designed in the Laboratory of Electromagnetic Fields, Institute of Petroleum Geology and Geophysics, Siberian Branch, Russian Academy of Sciences [Epov, 1990; Khabinov, 2009], were applied. The ERA program complex is a universal interactive system to work with the data of transient electromagnetic sounding. It should be noted that the EMS interpretation system is the development and extension to the ERA program complex for modern computers; it has good potential for using new NF TEMS modifications and new visualization techniques. Both systems allow processing and interpretation of the field data of active-source electromagnetic sounding using the models of laterally homogeneous media.

Construction of the basic interpretation model is the most important step in the computer processing of the NF TEMS measurements. We invoked additional a priori information for this purpose. The available data for the existing wells were analyzed and generalized.

Sedimentary filling of the depression took place at the same geological time over the entire territory; therefore, although the majority of the wells are located in the central part of the Chuya Depression, the same drilling data can be used also for the interpretation of measurements in the western part of the depression. The average drilling depth is relatively small (200–300 m). Only a few wells penetrated the Paleozoic basement [Nevedrova, 2001]. Examining the cross sections of these wells, we can trace the changes in the lithological composition of the medium with depth. The upper part of the cross section is composed of the coarsest gravel and pebble deposits that become finer-grained with depth. In the lowermost part of the section, the basement rocks are usually overlain by thin-bedded clays and close-grained sandstones without coarse-grained material. The same well data can be used to estimate the thickness of all lithological complexes and the total thickness of the sedimentary filling, which makes it possible to unambiguously determine the electric resistivity of the identified layers and, thus, to solve the questions concerning the equivalence of the geoelectrical models.

It was ascertained that the lowest resistivity values are typical for thin-layered formations: recent and Paleogene–Neogene clays, aleurolites, and argillites. The electrical resistivity (ER) of these sediments varies from 5 to 50 Ω m. Among the Paleogene–Neogene rocks, sandstones of the Tueryk suite, marls, and pitch coals are characterized by increased resistance values (to 200–300 Ω m). The rocks of the Tueryk and Koshagach suites are typically resistance-differentiated. The resistivity of the Paleozoic and Vendian sedimentary rocks ranges from 100 to 500 Ω m (except for limestones whose resistivity attains 1000 Ω m and higher). Magmatic rocks are characterized by the resistivity from 500 to 5000 Ω m.

Based on the analysis of a priori data, the main interpretation model was determined as a four-layer cross section with a high-resistivity upper part, a third well-conductive layer, and a nonconductive bottom layer. The apparent resistivity curves corresponding to this profile refer to the QH type ($\rho_1 > \rho_2 > \rho_3 < \rho_4$).

The interpretation of the major part of the NF TEMS data was carried out in the class of laterally stratified models. Primarily, this is associated with the high locality of the setup used for measurements [Rabinovich, 1987; *Metodicheskie*, ..., 1983]. Note that the induction setups with coaxial loops are least sensitive to nonhorizontal boundaries. The slopes of the transmitting and receiving loops caused by the topography of the Earth's surface have a negligible effect on the measurement errors.

The influence of the nonlateral boundaries and the scarps in the basement manifests itself as an evident distortion of individual segments in some sounding curves (usually, the right-hand branches of the apparent resistivity curves are distorted). These distortions had been thoroughly analyzed earlier [Kuznetsov, 1982; Nevedrova et al., 2006]. If there are no grounds to take into account the phenomenon of induced polarization, it is reasonable to determine the geoelectric parameters of the cross section from the curve including the vicinity of the minimum and rejecting the major part of the right-hand side branch (otherwise we would not be able to reliably estimate the resistivity of the reference horizon).

In order to exemplify the data interpretation, we consider one of the NF TEMS field curves for profile 3 and the corresponding geoelectrical model (Fig. 2). The NF TEMS curve 102 completely corresponds to the type described. The minimum of the curve indicates the presence of a conducting layer in the section, which overlies the reference geoelectrical horizon. The inversion of the field data yielded a four-layer model with the resistivity of the third (lowest-ohmic) layer of 31 Ω m; therefore, these sediments can be referred to as the Koshagach suite. A shallower layer with resistivity of 196 Ω m characterizes the Tueryk suite. The uppermost layer is characterized by the highest resistivity attaining 1100 Ω m. It should be noted that the resistivity of the upper layer strongly varies within the study area mainly depending on the content of the coarse deposits, permafrost, and the water content. The typical distortion of the right-hand branch of the NF TEMS curve 102 is apparent. The curves of apparent resistivity calculated for the stratified homogenous media with a nonconductive basement and plotted in bilogarithmic coordinates are known to approach a line inclined at an angle of approximately 63° to the horizontal axis with increas-

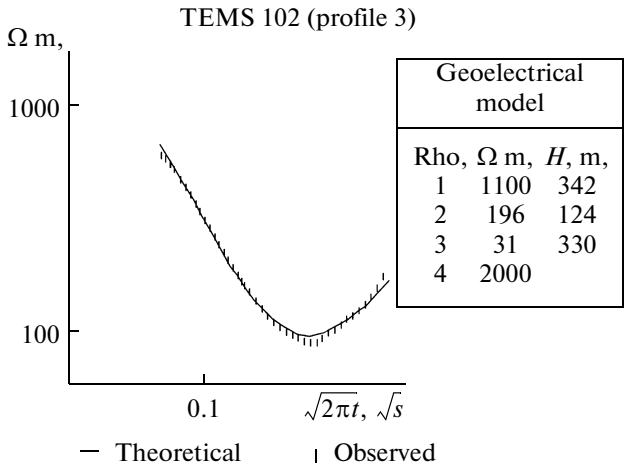

Fig. 2. Field data, synthetic curve, and geoelectrical model at NF TEMS 102 (profile 3).

ing period. The distorted curves are usually characterized by much higher angles. Therefore, a segment of the right-hand branch of the NF TEMS curve 102 was disregarded in the determination of the geoelectric parameters of the cross section, and the electric resistivity of the reference horizon was estimated conditionally.

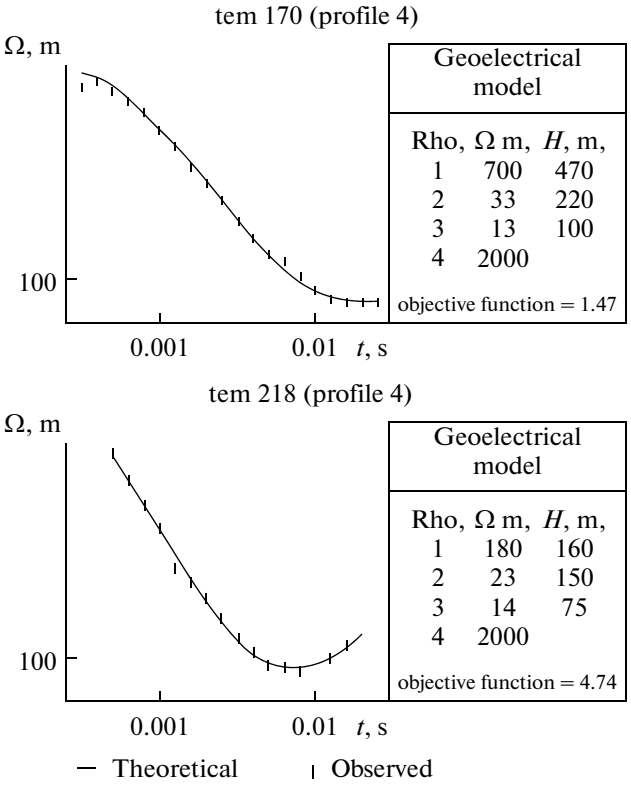

Fig. 3. Field data, synthetic curves, and geoelectrical models at NF TEMS 170 and 218 (profile 4).

Now, we turn to Fig. 3, which displays the field NF TEMS curves for profile 4. This profile has a longer extension than profile 3; it reflects the key features of the tectonic depression. Here, several supposed fault structures are distinguished. The geoelectrical NF TEMS models 170 and 218 also contain four layers, although the resistivity of these layers slightly differs from the values for the profile3. NF TEMS station 218 is located in the bed of the Chagan–Uzun River. The sediments in the upper part of the cross section are most probably filled with water; their resistivity is less than 200 Ω m. The farther away from the river the larger the resistivity of the layer. At station 170 it is 700 Ω m. Layers 2 and 3 are also composed of higher-conductive sediments than those in profile 3. This is also determined by the geological conditions: most probably, the sediments deposited closer to the center of the depression are thinner-layered.

The procedure for processing and interpretation of the NF TEMS data acquired in the tectonic depressions has been already described in sufficient detail in several works [Nevedrova, 2001; Nevedrova et al., 2006]. Therefore, in the present paper we will focus on the more detailed interpretation for the MTS method, which has been first applied for the medium-scale survey in the Mountain Altai, and on the joint interpretation of these two electromagnetic methods.

MTS Method

We start with the stage of qualitative interpretation, when the dimensionality of the geological model is selected. The real distribution of the MT field is known to depend on all elements of the medium being sounded, both vertical and lateral. Therefore, an important stage of interpretation is the analysis of magnetotelluric data, which allows us to construct the interpretation model of the region under study. Here, the leading role belongs to the polar diagrams of magnetotelluric tensor $\hat{Z}$, which represent the dependence of the MT responses on their orientation [Berdichevsky and Logunovich, 2005], and the magnetotelluric parameters, namely, the heterogeneity parameter N [Berdichevsky et al., 1997], the skew [Swift, 1967], and phase-sensitive skew η [Bahr, 1988].

The analysis of the polar diagrams of the impedance tensor for the western part of the Chuya Depression showed that, generally, the cross section here is quasi-two-dimensional (Fig. 4). In the two-dimensional model striking along the X axis

$$\hat{Z} = \begin{vmatrix} 0 & Z^{\parallel} \\ -Z^{\perp} & 0 \end{vmatrix},$$

where the longitudinal and the transverse impedances $Z^{\parallel}$ and $Z^{\perp}$ are the principal values of the impedance tensor. The apparent resistivity curves calculated along the principal values of the impedance tensor are longi-

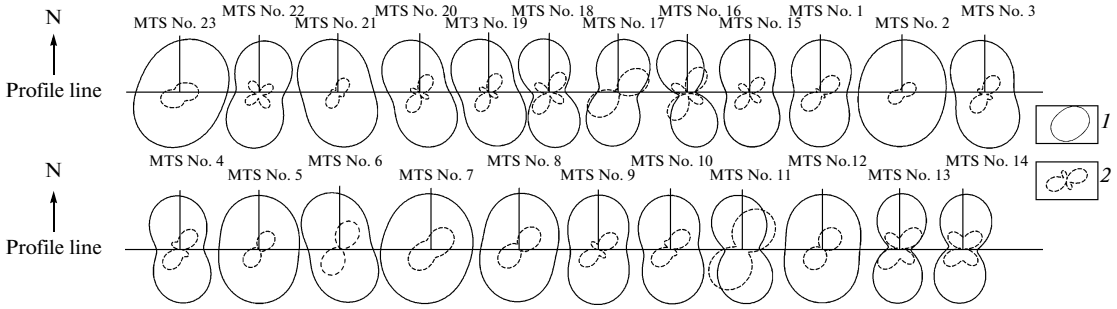

Fig. 4. Polar diagrams of the impedance tensor $|\hat{Z}|$ for the period $T = 1$ s: 1 polar diagram $|Z_{xy}|$; *2* polar diagram $|Z_{xx}|$.

tudinal ($\rho^{\parallel}$) and transverse ($\rho^{\perp}$) with respect to the strike of the geological structures. The validity of the choice of the quasi-two-dimensional model is supported by the analysis of magnetotelluric parameters N, skew, and η (Fig. 5), which are calculated as

$$N = \left|\sqrt{1 - 4\frac{Z_{xx}Z_{yy} - Z_{xy}Z_{yx}}{(Z_{xy} - Z_{yx})^2}}\right|,$$

$$\text{skew} = \left|\frac{Z_{xx} + Z_{xy}}{Z_{xy} - Z_{yx}}\right|,$$

$$\eta = \frac{\sqrt{0.5\left|\text{Im}(Z_{xy}Z_{yy}^* + Z_{xx}Z_{yx}^*)\right|}}{|Z_{xy} - Z_{yx}|},$$

where * denotes a complex conjugation.

It is known that in the laterally homogeneous model

$$N = \text{skew} = \eta.$$

The deviation of N from 0 characterizes the lateral heterogeneity of the medium. In a two-dimension model, $N \neq 0$, while skew $= \eta = 0$. In a three-dimensional model, all the three parameters are nonzero. As follows from Fig. 5, at high frequencies ($T \ll 1$), the heterogeneity parameter N is less than 0.2, which indicates that one-dimensional estimations are applicable to assess the resistivity of the uppermost portion of the geoelectric cross section. Starting with the periods $T > 1$ s, the value of N increases to 0.4–0.5, and with decreasing frequency ($T > 100$ s), it increases up to 0.7. High values of N correspond to an enhanced skew that vary from 0.05 to 0.1 at long periods and attain 0.6 at short periods. With increasing frequency, the phase-sensitive skew η increases, which, according to Bahr [Bahr, 1988], is evidence of the absence of local three-dimensional inhomogeneities in the upper part of the section. There are two zones where η decreases to 0.08 over the periods from 1 to 160 s. One is located in the region of MTS stations nos. 18–15 and corresponds to the zone of the deep fault; another (MTS sites nos. 6–14) apparently reflects the fault structures of the depression itself and its boundary with the Chagan–Uzun block (Fig. 5).

Thus, the geoelectrical section of the study region can be regarded as a regional two-dimension structure containing local three-dimensional inclusions in the middle and upper crust. The comparison between the MTS and NF TEMS data described in the next section of the paper also confirms the two-dimensionality of the studied geoelectric section.

There are various recommendations and conclusions concerning which of the MTS curves are the most informative in the 1D inversion [Kovtun, 2004; Spichak, 1999; *Sovremennye*..., 2009]. The results discussed in the present paper were obtained using the longitudinal curves. They were selected because in the study region the longitudinal MTS curves agree with the NF TEMS curves, after having been overlapped by the curves with which these MTS curves were interpreted using the one-dimensional programs.

The selection of longitudinal (quasi-longitudinal) curves over the study region was implemented in the Line-Inter-MT program package, using which the profile processing and interpretation of the MTS data were carried out. Figure 6 shows the typical longitudinal curves calculated for the western part of the Chuya Depression.

The main task of the further profile processing of the results yielded by one-dimensional inversion is correction for the S effect and preparation of the data for constructing the final geoelectrical sections.

As is well-known, in the general case, if the medium contains inhomogeneous inclusions at all depth levels of the geoelectric cross section, the influence of the S effect becomes stronger with the increasing depth of the MT field's penetration into the Earth, since ever new geoelectrical heterogeneities start affecting the volume captured by the field.

This situation is typical in the region of study; i.e., the discrepancy in the ρ_T curves increases with the increasing period of the electromagnetic wave.

Under these conditions, different corrections are needed to compensate for the action of the S effect in different depth intervals of the geoelectrical cross section. This procedure of introducing such corrections has been implemented in the Line-Inter-TM program complex. The key point in this procedure is calcula-

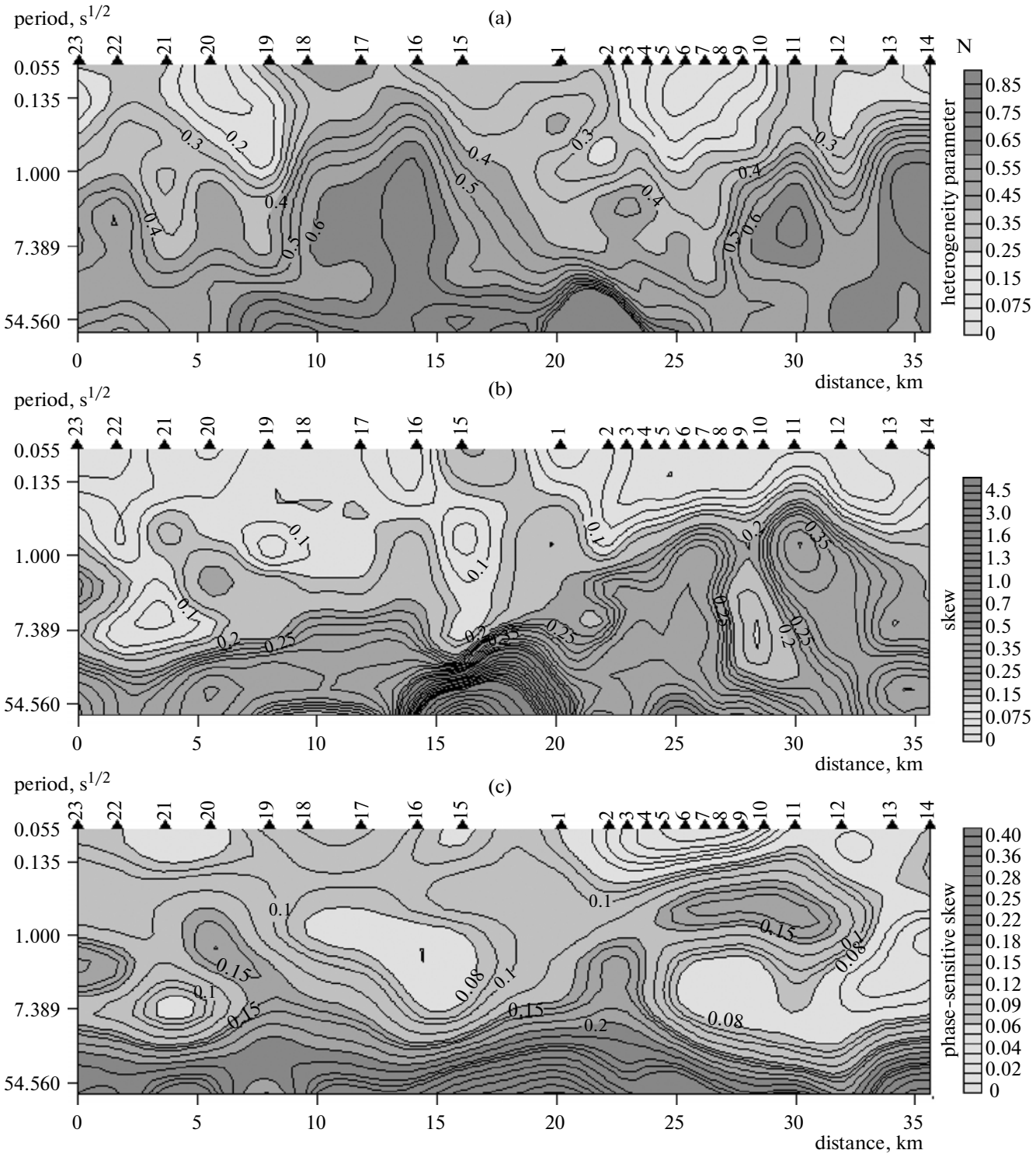

Fig. 5. Frequency sections of the magnetotelluric parameters: (a) heterogeneity parameter N; (b) skew; (c) phase-sensitive skew η.

tion of the quasi-longitudinal component not impacted by the S effect. Here, when analyzing the profile measurements, the allowed impedance gradients for a certain penetration depth of the MT field (i.e., with certain assumptions, for the impedance values at a certain period) are restricted by specific-degree polynomial constraints. In this case, if the impedance values calculated for the given profile at a certain period (frequency) are approximated by the fitted polynomial, all deviations from this approxima-

tion should be regarded as geological noise (mainly in the form of an S effect), and the corresponding corrections should be introduced to reduce the values of the measured impedances to the polynomial values. Then, it is necessary to introduce corrections to the results of the one-dimensional inversion. Actually, this is equivalent to the procedure of filtering with different filter parameters (windows) for different depths.

The work with the results of one-dimensional inversion in the profile processing module of the Line–Inter–MT package is conducted in the model that is recalculated after introducing the corrections for the S effect. Here, the position of the corrected theoretical and observed curves relative to L. L. Vanyan's normal curve and the global MTS curve can be estimated for each observation point (Fig. 7). Such an estimation is a good criterion when working with the geoelectric section up to a depth below 200 km, where the main target of the study is the uppermost conductive mantle.

The Technique of a Joint Interpretation of the Electromagnetic Sounding Data (MTS and NF TEM)

Without the combination of MTS with other types of electromagnetic soundings, one cannot solve issues regarding the geoelectric effects of the upper layers; determination of the model geoelectrical section in the vicinity of the observation points; and analysis of the impact of local inhomogeneities that are contained in the sedimentary cover and have different conductivities; and analysis of some soundings that carry information about the deep structure of the region.

The optimal combination is NF TEMS and MTS. NF TEMS and MTS should be carried out in such a manner that they provide overlapping intervals within which the soundings respond to the same parameters of the geoelectric section.

In the joint interpretation of the NF TEMS and MTS, the problem arises on how to align the curves corresponding to the different types of electromagnetic sounding. The most suitable method is alignment of the curves with reference to the level of the apparent resistivity and the S and H parameters, if the latter are the same for the overlap region. The curves are aligned in the following way:

(1) the total conductivity S_Σ is calculated from the NF TEMS curve yielded by inversion;

(2) the value $\sqrt{2\pi t}$ is determined from the analytical expression $S = 452\sqrt{\frac{2\pi t}{\rho}}$ at the fixed resistivity at which the curves are aligned with each other. An asymptote passing through the intersection of ρ and $\sqrt{2\pi t}$ is drawn at an angle of 63°;

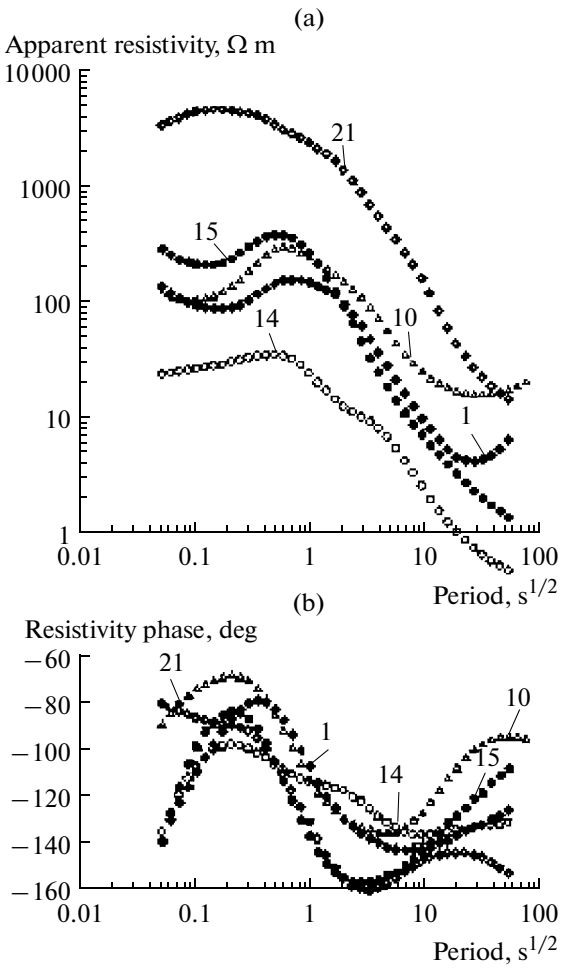

Fig. 6. Typical longitudinal MTS curves along the profile I–I: (a) amplitudinal; (b) phase.

(3) according to the relation $S = 356\sqrt{\frac{T}{\rho}}$, $\sqrt{T}$, is calculated with the same value of resistivity corresponding to the S_Σ value determined from the NF TEMS curve. An asymptote passing through the intersection of ρ and $\sqrt{T}$ is drawn at an angle of 63°;

(4) the curves are aligned in the selected resistivity until they intersect the asymptotic lines. The left-hand part of the MTS curve is extended using the parameters of the NF TEMS curve in terms of the ρ and $\sqrt{T}$ coordinates, after which the resulting curve can be interpreted as a single MTS curve. An example of the NF TEMS and MTS curves aligned at one point of profile no. 3 are shown in Fig. 8.

INTERPRETATION OF THE NF TEMS AND MTS FIELD DATA: THE RESULTS

We start with discussing the results of the joint interpretation of the NF TEMS and MTS data for

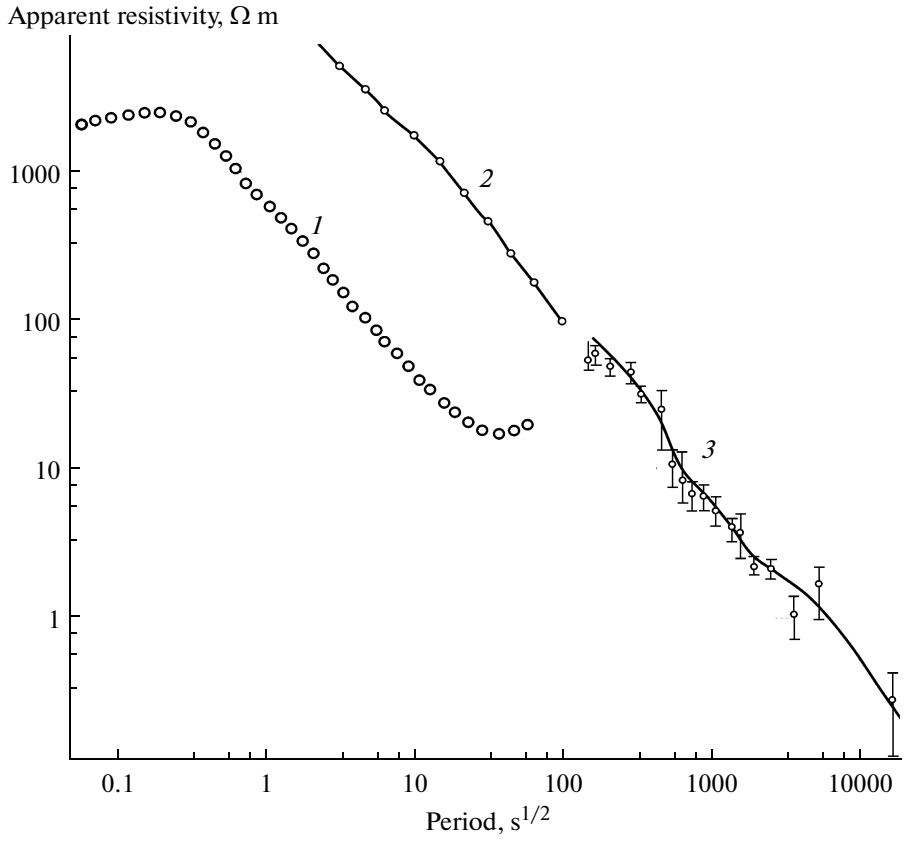

Fig. 7. Position of the observed MTS curve relative to the normal Vanyan's curve and the global magnetovariational sounding curve. (*1*) Vanyan's global curve; (*2*) MVS; (*3*) experimental data.

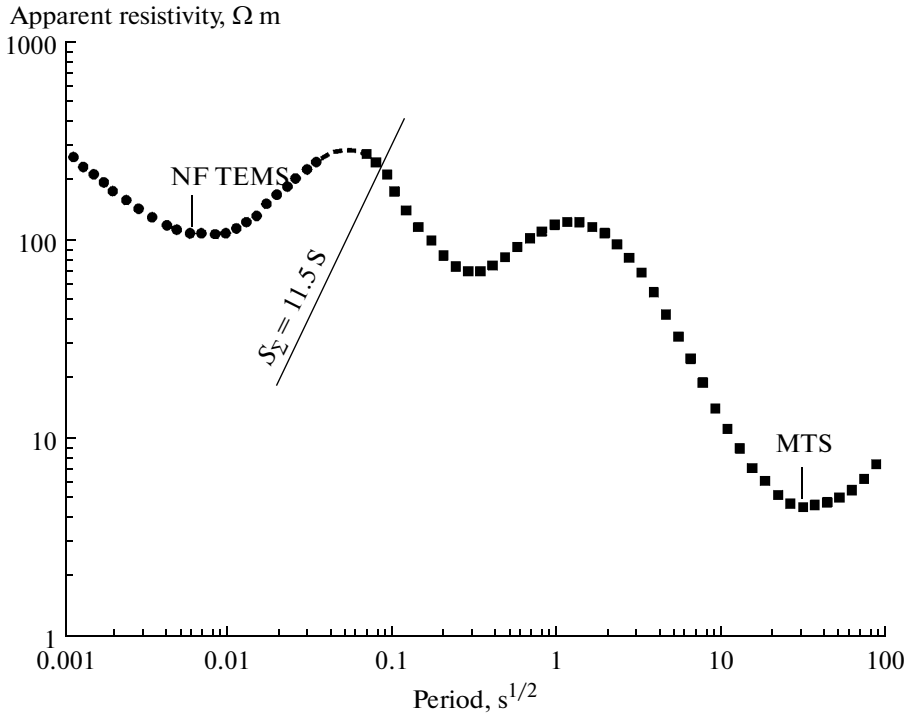

Fig. 8. Example of alignment of the NF TEMS and MTS curves at the single sounding site.

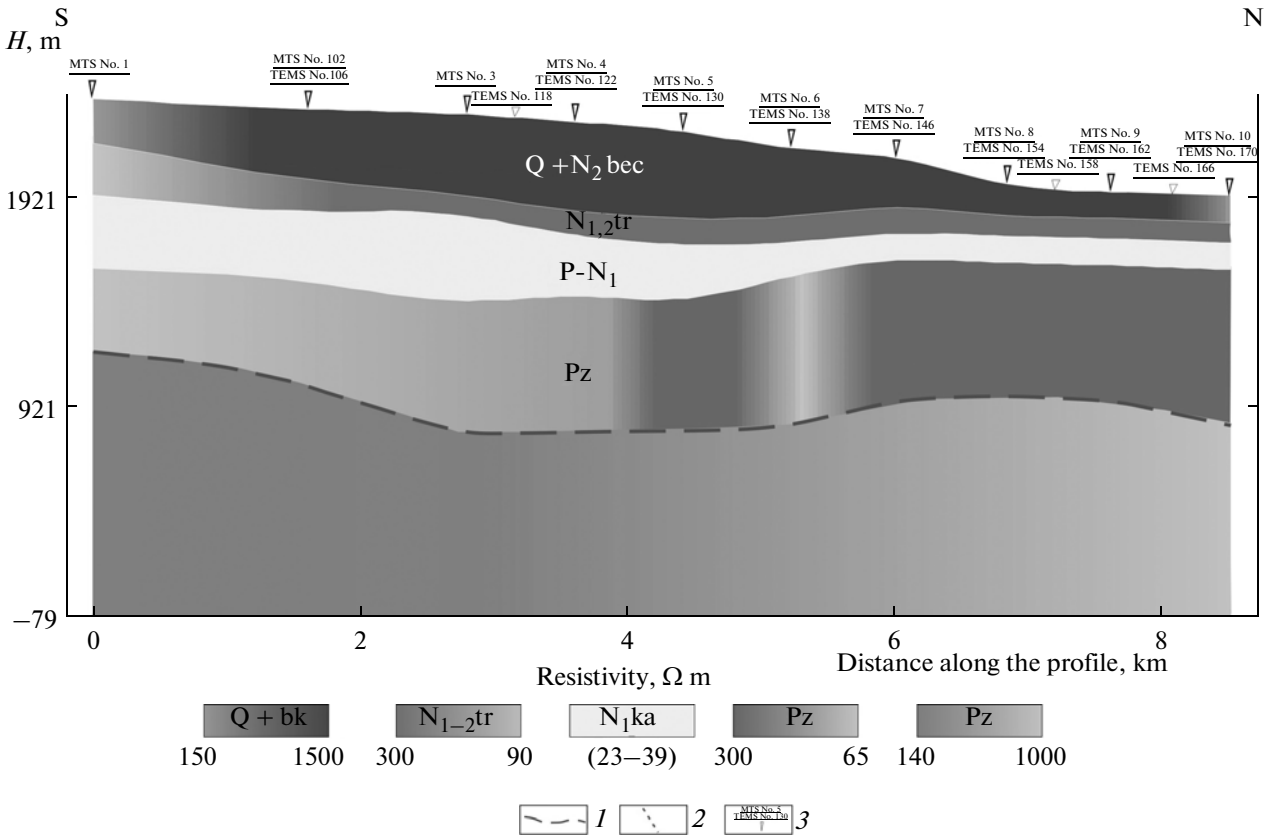

Fig. 9. Geoelectrical section along profile 3, according to the joint interpretation of NF TEMS and MTS data: *1* geoelectrical boundary in the basement; *2* supposed faults; *3* NF TEMS and MTS sites.

profile no. 3 (NF TEMS), where almost all measurement points were coincident with the MTS observation points. The geoelectric section along this profile is shown in Fig. 9. We note the main distinctive features of this section. The layer with the highest conductivity overlying the Paleozoic high-resistivity sediments is consistent in resistivity, which in the central part of the layer varies within a narrow interval from 23 to 27 Ω m (NF TEMS 118–138). In the northern part of the profile, the thickness of this layer sharply decreases, and the resistivity increases (NF TEMS 138–170). The layer attributed to the Tueryk suite is consistent in terms of thickness and resistivity. The uppermost horizon with variable thickness has the highest resistivity, which is due to its lithological composition, namely, the presence of moraine coarse deposits.

The most fascinating result is that for the first time a geoelectrical boundary (shown in Fig. 9 by the dashed line) is sufficiently reliably identified in the Paleozoic sediments at a depth of more than 1000 m. It should be noted that in the northern part of the profile this boundary was independently revealed using the NF TEMS data. Recognition of this boundary shows that the geological history of the Paleozoic formation of the depression was more complex than had been believed before. At present, there are only some hypotheses on which rocks are responsible for the change in the electrical properties of the rocks at the given depth in the upper part of the basement. An interpretation of this effect is the subject for further research.

Now, we consider the deep structure of the lithosphere according to the MTS data on profile I–I partly coincident with the NF TEMS profile no. 3. Two regions with different geoelectrical characteristics are distinguished in the cross section of the lithosphere (Fig. 10). The southwest region (MTS point nos. 23–17) reflects the features of the Earth's crust of the South Chuya Range that is composed here of dyke belts of alkaline basalts and mica lamprophyres of the Chuya complex [Vladimirov et al., 2005; 1997]. According to the MTS data, the resistivity of the upper and middle crust of the South Chuya Range is at least 5000 Ω m. This region is marked also by increased gravity (Δg) and magnetic (ΔT) fields (Fig. 10). The middle crust here contains a conductive layer at a depth of 18–20 km; the resistivity of the layer is at most 100 Ω m. These parameters correspond to the normal geoelectrical section of tectonically active regions. The other region overlaps the central and the northeast parts of the profile and corresponds to the Chuya Depression in a plane. From the southeast

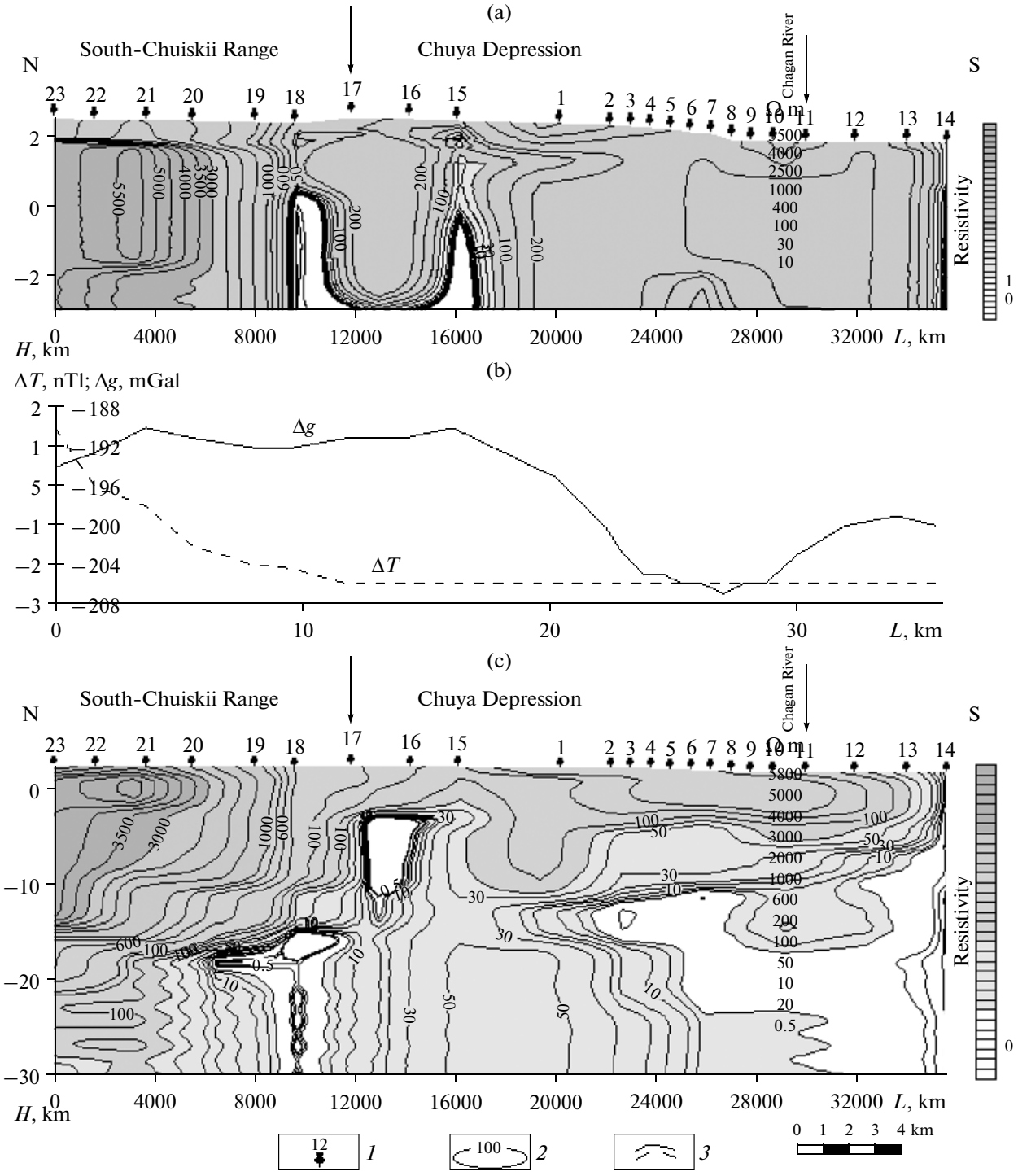

Fig. 10. (a) Geoelectrical section of the sedimentary cover along profile I–I; (a) upper part of the geoelectric sectorn; (b) graphs of gravity and magnetic field; (c) deep geoelectrical section along profile I–I: *1* sites of magnetotelluric sounding; *2* equiresistivity contours in Ω m; *3* graphs of gravity and magnetic fields.

(MTS nos. 18, 17), the Chuya Depression is bounded by an inclined conductive zone (with the resistivity of a few Ω m), which outlines the tectonic boundary of the folded system of the South Chuya Range. Within the Chuya Depression, the conductive crustal layer is elevated to a depth of approximately 12 km (to 8–10 km in the northern part of the profile), and the resistivity of this layer decreases to 5–10 Ω m.

Finally, we consider the geoelectrical section along profile no. 4, reconstructed using the NF TEMS data

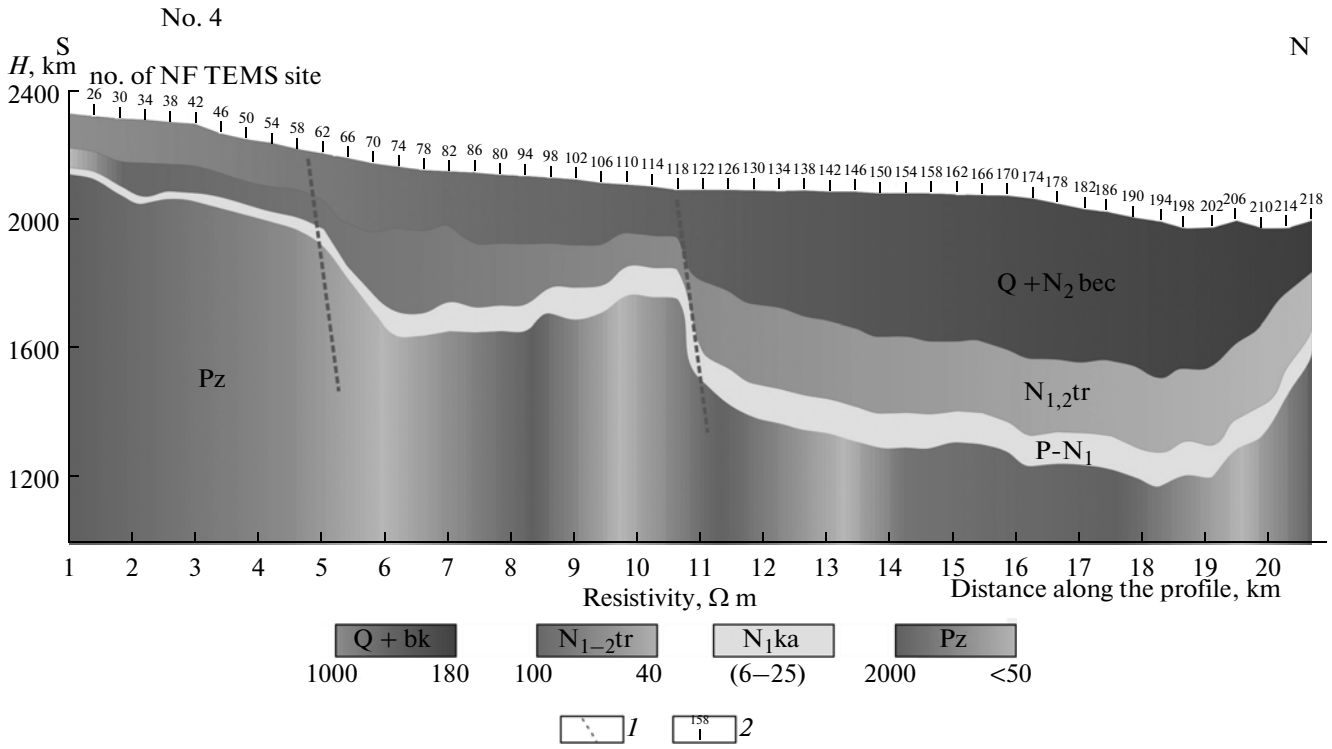

Fig. 11. Geoelectrical section along profile 4, according to the NF TEMS data: *1* supposed faults; *2* NF TEMS and MTS sites.

(Fig. 11). The profile intersects the western part of the depression practically from south to north, starting near the southern mountain frame and ending near the Chagan–Uzun block in the north. Two supposed faults are identified in the profile. The faults are marked by sharp benches of the basement and are rather distinctly traced by the steps in the sedimentary cover at shallower depths. Similar faults were recognized on the neighboring profile no. 5 as well. The faults are the most important tectonic units, which ultimately determine the fault–block structure of the intermontane depressions.

The comparison of the deep structure of the lithosphere with the data about the hypocenters of the registered earthquakes suggests that the elevated top of the intracrustal conducting layer may separate the upper rigid block from the more plastic fluid-saturated lower part of the section. The interface between these zones is just the place where bulk release of accumulated strains occurs.

Similar results were obtained at the segment of the Tashanta–Kosh–Agach–Teeli regional profile acquired by the Krasnoyarsk Research Institute of Geology and Mineral Resources. The works were carried out in the scope of the Federal program "Geophysical Studies of the Deep Structure of the Altai–Sayan Folded Region with the Application of Seismic and Electromagnetic Methods." Elevation of the crustal layer to a depth of 8–12 km in the regions of known focal zones of earthquakes (the Altai and Shapshal) has been also identified in these survey results. The most pronounced changes in the parameters of the crustal conducting layer are revealed within the Altai focal zone. A reduction in the longitudinal resistivity of this layer to 10–20 Ω m is observed; the upper boundary of the layer in this region is maximally elevated to a depth of 8 km.

The time variations in the fluid system and geophysical inhomogeneities of the consolidated crust depend on the geodynamic situation and, therefore, on the thermodynamic conditions. The variations in the resistivity of the crustal conducting layer before and after a series of weak and moderate earthquakes, which have been recorded during several months in the Bishkek test site, were interpreted as the change in the fluid saturation of the conducting layer [Kisin, 2001].

Changes in the parameters of the crustal conducting layer in seismically active areas were noted in many regions in Russia and abroad. Thus, in Hungary the depth to the conductor within the Trans–Dunai seismically active region reduces to 5.5–7 km. This region is marked by the most intense earthquakes. Interesting data were obtained in the Krasnoslobodsk geodynamic test site located in the zone of the eastern marginal deep fault of the Central–Belarussian suture zone, being the junction zone between the Fennoscandian and the Sarmat geosegments. According to the mag-

netotelluric sounding data, here the depth to the conductive layer is 10 km in the central part and 18 km in the marginal part of the region; these changes in the depth are accompanied by a simultaneous increase in conductivity from 50 to 200 Siemens.

Thus, the change in the geoelectric parameters (the depth and the resistivity) of the crustal conductive layer may become one of the criteria for assessment of the nature of deep seismicity according to the electric data.

The results of detailed complex electromagnetic studies allowed us to advance our understanding of the geoelectrical structure of the sedimentary cover and the Earth's crust in the complex tectonic environment of the epicentral zone of the Chuya earthquake. New data about the deep geoelectrical structure of the Earth's crust have been obtained; a detailed cross section of the sedimentary cover is constructed for the western part of the Chuya Depression.

CONCLUSIONS

1. The combination of the NF TEMS and MTS methods allows one to select a qualitative interpretation for either the transverse or longitudinal MTS curve, which is least distorted by the influence of the upper part of the cross section.

2. The coincidence of the NF TEMS parameters and the parameters of one of the MTS curves can serve as a criterion in the selection of the model of a deep geoelectrical section of the region.

3. A combined approach to the processing of the field data improves the reliability of the obtained geoelectrical cross sections.

4. The main advantages of each of the methods are demonstrated. The NF TEMS data provide a more detailed imaging of the upper part of the geoelectric cross section (up to 1.5–2 km), while the MTS data yield information about the deep structure of the lithosphere.

5. According to the MTS data, the depths to the crustal conducting layer are estimated. It is found that in the epicentral zone of the Chuya earthquake the depth to the crustal conductor is reduced to 8–10 km.

6. Identification of the geoelectrical boundary in the upper part of the basement in the western part of the Chuya Depression according to the NF TEMS and MTS data indicates that the structure and geological history of the Chuya Depression in the Mountain Altai is more complex than it was believed earlier.

ACKNOWLEDGMENTS

This study was supported by the Targeted Federal Program "Academic and Teaching Staff of Innovative Russia for 2009–2013" (State Contract no. P 792).

REFERENCES

Bahr, K., Interpretation of Magnetotelluric Impedance Tensor: Regional Induction and Local Telluric Distortion, *J. Geophys.*, 1988, pp. 119–127.

Berdichevsky, M.N., Dmitriev, V.I., Novikov, D.B., and Pastutsan, V.V., *Analiz i interpretatsiya magnitotellurichеskikh dannykh* (Analysis and Interpretation of Magnetotelluric Data), Moscow: Dialog MGU, 1997.

Berdichevsky, M.N. and Logunovich, R.F., Magnitotelluricheskie polyarnye diagrammy (Magnetotelluric Polar Diagrams), *Fiz. Zemli,* 2005, no. 10, pp. 66–78 [*Izv. Phys. Earth* (Engl. Transl.), 2005, vol. 41, no. 10, pp. 832–-843].

Epov, M.I., Dashevskii, Yu.A., and El'tsov, I.N., *Avtomatizirovannaya interpretatsiya elektromagnitnykh zondirovanii* (Automated Interpretation of Electromagnetic Sounding), Novosibirsk: Inst. geologii i geofiz. SO AN SSSR, 1990.

Khabinov, O.G., Chalov, I.A., Vlasov, A.A., and Antonov, E.Yu., EMS System for Interpretation of TEM Sounding Data, in *Geosibir'-2009* (Geo–Siberia 2009), Novosibirsk, 2009, pp. 108–113.

Kisin, I.G., The Fluid System and Geophysical Heterogeneities of Consolidated Earth Crust of the Continents, *Vestnik OGGGN RAN*, 2001, no. 2, pp. 1–19.

Kovtun, A.A. Vagin, S.A., et al., Structural Features of Karelian Region According to the Geoelectrical Data, in *Glubinnoe stroenie i seismichnost'Karel'skogo regiona i ego obramleniya* (Deep Structure and Seismicity of Karelia and its Margins), Sharov, N.V., Ed., Petrozavodsk: KarNTs RAN, 2004.

Kuznetsov, A.N., Distorting Effects in the Electromagnetic Sounding of Laterally Inhomogeneous Media using Active Sources, *Izv. Akad. Nauk SSSR, Fiz. Zemli*, 1982, no. 2, pp. 67–78.

Metodicheskie rekomendatsii po analizu zondirovanii stanovleniem polya v blizhnei zone v gorizontal'no-neodnorodnykh sredakh (Methodical Recommendations on the Analysis of Near-Field Transient Electromagnetic Sounding Data in Laterally Inhomogeneous Media), Rabinovich, B.I. and Finogeev, V.V., Eds., Novosibirsk: Nauka, 1983.

Nevedrova, N.N., Epov, M.I., Antonov, E.Yu., and Dashevskii, Yu.A., Reconstruction of the Deep Structure of the Chuya Depression in the Mountain Altai According to the Electromagnetic Sounding Data), *Geol. Geofiz.*, 2001, vol. 41, no. 9, pp. 1399–1416.

Nevedrova, N.N. and Antonov, E.Yu., Electromagnetic Methods for Studying the Structure and Geodynamics of the Chuya Depression in the Mountain Altai, in *Altaiskoe (Chuiskoe) Zemletryasenie: Prognozy, Kharakteristiki, Posledstviya* (The Altai (Chuya) Earthquake: Prediction, Characteristics, Aftermath), Gorno–Altaisk: Gorno-Altaisk. Gos. Univ., 2004, pp. 37–47.

Nevedrova, N.N., Babushkin, S.M., and Dashevskii, Yu.A., Geoelectric Studies in the Mountain Altai in the Context of Chuya Earthquake, 2003, *Vestn. Natl. Yadern. Tsentr. Resp. Kazakhstan*, 2006a, no. 2, pp. 161–166.

Nevedrova, N.N., Epov, M.I., and Antonov, E.Yu., Allowance for Typical Distortions of the field TEM Curves in Seismically Active Regions, *Geofiz. Vestn.*, 2006b, no. 6, pp. 8–14.

Rabinovich, B.I., *Osnovy metoda zondirovanii stanovleniem polya v blizhnei zone* (Principles of Near-Field Transient Electromagnetic Sounding), Irkutsk: Irkutsk. politekhnich. inst., 1987.

Sovremennye metody izmereniya, obrabotki i interpretatsii elektromagnitnykh dannykh (Modern Methods for Measuring, Pro-

cessing, and Interpretation of Electromagnetic Data), Spichak, V.V., Ed., Moscow: LIBROKOM, 2009.

Spichak, V.V., *Magnitotellurichеskie polya v trekhmernykh modelyakh geoelektriki* (Magnetotelluric Fields in Three-Dimensional Geoelectric Models), Moscow: Nauchnyi Mir, 1999.

Swift, C.M., A Magnetotelluric Investigation of an Electrical Conductivity Anomaly in the Southwestern United States, *Dissertation*, Cambridge: MIT, 1967.

Vanyan, L.L., Berdichevsky, M.N., Pushkarev, P.Yu., and Romanyuk, T.V., Geoelektricheskaya model' kaskadnoi subduktsionnoi zony (A Geoelectric Model of the Cascadia Subduction Zone), *Fiz. Zemli*, 2002, no. 10, pp. 23–53 [*Izv. Phys. Earth* (Engl. Transl.), 2002, vol. 38, no. 10, pp. 816–845].

Vladimirov, A.G., Ponomareva, A.P., et al., Late Paleozoic–Early Mesozoic Granitoid Magmatism in Altai, *Geol. Geofiz.*, 1997, vol. 38, no. 4, pp. 715–730.

Vladimirov, A.G., Kruk, N.N., Polyanskii, O.P., et al., Correlation of the Hercynian Deformations, Sedimentation and Magmatism of the Altai Collision System as a Manifestation of the Plate- and Plum Tectonics, in *Problemy tektoniki Tsentral'noi Azii* (Tectonic Problems of the Central Asia), Moscow: GEOS, 2005, pp. 277–308.